MODEL HIERARCHIES FOR CELL AGGREGATION BY CHEMOTAXIS

FABIO CHALUB, YASMIN DOLAK-STRUSS, PETER MARKOWICH, DIETMAR OELZ, CHRISTIAN SCHMEISER, AND ALEXANDER SOREFF

(Day Month Year) (Day Month Year) (xxxxxxxxxx)

Abstract. We present PDE (partial differential equation) model hierarchies for the chemotactically driven motion of biological cells. Starting from stochastic differential models we derive a kinetic formulation of cell motion coupled to diffusion equations for the chemoattractants. Also we derive a fluid dynamic (macroscopic) Keller-Segel type chemotaxis model by scaling limit procedures. We review rigorous convergence results and discuss finite-time blow-up of Keller-Segel type systems. Finally, recently developed PDE-models for the motion of Leukocytes in the presence of multiple chemoattractants and of the slime mold *Dictyostelium Discoideum* are reviewed.

Chemotaxis, Keller-Segel model, Moment expansion, Macroscopic limit.
AMS Subject Classification: 92C17

1. Introduction

Many fundamental processes in biology and physiology depend on the ability of cells to react to external cues. Especially chemotaxis, the biased locomotion of cells towards chemical gradients, plays an important role for numerous biological systems. Chemotaxis models are applied to embryogenesis and wound healing. Moreover they are used in the modelling and simulation of the immune response system and of cell aggregation, examples of which will be presented in the sequel. Chemotaxis is also of major importance in tumor biology. A chemotaxis model was employed e.g. in [2] to describe tumor induced endothelial cell migration. A further example is [37] where a system of reaction-drift-diffusion equations has been used to simulate tumor invasion. By quantifying haptotaxis and chemotaxis the authors could show that the "therapeutic use of protease inhibitors against tumors expressing high levels of matrix metalloproteinase could produce an augmentation of invasion".

In 1970, E. Keller and L.A. Segel derived a model for chemotaxis that should become one of the best-studied models in mathematical biology [25]. Consisting of an equation for the cell density $\rho = \rho(x,t)$ coupled to the concentration $S = S(x,t)$ of a chemical ($x \in \mathbb{R}^n$, $n = 2$ or 3 denotes the position variable and $t > 0$ time) the cell are attracted to, it reads

$$\frac{\partial \rho}{\partial t} + \nabla \cdot (\chi(\rho, S)\rho \nabla S) = \nabla \cdot (D_\rho(\rho, S)\nabla \rho) \tag{1}$$

$$\frac{\partial S}{\partial t} = \nabla \cdot (D_S(\rho, S)\nabla S) + g(\rho, S), \tag{2}$$

where the positive function $\chi(\rho, S)$ is the so-called chemotactic sensitivity. The positive functions $D_\rho(\rho, S)$ and $D_S(\rho, S)$ denote the diffusivities of the cells and the chemical and $g(\rho, S)$ describes production and degradation of the chemical, depending on whether $g(\rho, S)$ takes positive or negative values. Actually, equation (1) was already derived by Patlak [34] in 1953, but nevertheless, system (1), (2) has mostly become known as the Keller-Segel model for chemotaxis.

This model, originally derived to describe aggregation of the slime mold amoeba *Dictyostelium discoideum* (Dd), has been successfully used in various contexts. However, what we shall call the classical Keller-Segel model, with constant coefficients χ and D_ρ and a linear function $g(\rho, S) = \alpha\rho - \beta S$, is often not sufficient to describe biological phenomena in a satisfactory way. Additional information can be incorporated in 'microscopic' models describing chemotaxis on the level of individual cells. This paper reviews a modelling framework, where the movement of an individual cell is described as a stochastic process depending on a finite number of 'internal degrees of freedom', i.e., quantities describing the internal state of a cell. This leads to high dimensional partial differential equations for the cell distribution functions, whose complexity is in general prohibitive for numerical simulations. Therefore, systematic simplification procedures are required, two of which are presented in the following section. The first one, here called the 'macroscopic limit' provides a dimension reduction by reducing the position-velocity state space to position space. In terms of stochastic processes it deals with a scaling limit, where a velocity jump process is reduced to a Brownian motion with drift. In terms of equations for probability distributions, kinetic transport equations are reduced to drift-diffusion equations. The second simplification replaces the dynamics of distributions with respect to the internal quantities by equations for their expectation values. The methodology, here termed 'moment expansion', consists in using heuristic closure assumptions in moment equations. Applications of these simplification steps lead to model hierarchies with Keller-Segel type models at the bottom end and, thus, to systematic extensions based on detailed knowledge on individual cell behaviour.

The remaining sections review several recent mathematical and modelling contributions within this framework, in particular concerning models for cell aggregation by chemotaxis.

Section 3 deals with rigorous justifications of macroscopic limits, i.e., the derivation of fluid models of the Keller-Segel type from kinetic transport equations. The fluid models are diffusive as described above, if the dominant microscopic turning processes are without directional preference. If, on the other hand, a strong orientation is produced already on the microscopic level, then the macroscopic limit produces a purely convective fluid model.

The above mentioned classical Keller-Segel model features a description of aggregation in a very distinctive way. Under appropriate conditions, blow up in finite time occurs, i.e. concentration of the cell density. The derivation of criteria for global existence vs. blow up of solutions has received a lot of attention. Of particular interest is the continuation of solutions after aggregation to describe the interaction of aggregates and the dynamics of nonaggregated cells. A recent approach is the introduction of regularized models possessing global smooth solutions. In section 4 we present, after a short review on results concerning blow-up, models featuring global existence of solutions.

In the last two sections, we shall discuss extensions of the Keller-Segel model which are motivated by experimental results. In sections 5, we present a model for the chemotactically directed migration of neutrophil leukocytes, reproducing the multistep navigation by memory effects investigated experimentally by E.F. Foxman, J.J. Campbell and E.C. Butcher in [13]. The crucial idea of this model is that the chemotactic sensitivity is not a constant, but a time-dependent function that adapts according to the chemical signal.

In section 6, we review a model describing the aggregation of the slime mold *Dictyostelium discoideum*. This process is controlled by chemotaxis: certain cells ("pacemakers") emit the chemical cAMP in a periodic fashion, and surrounding cells relay the signal by secreting it themselves while moving towards the source. Since the chemical spreads in the form of virtually symmetric wave trains, aggregation would not be observed if the cell only followed the chemical gradient (*chemotactic wave paradox*): they would actually follow the wave, away from the aggregation site. Several authors have proposed resolutions to this paradoxon (for instance Höfer *et al.* [20], or Rappel [44]), and it is often assumed that cells become either desensitized at the wave peak or that some sort of polarity is established that prevents the cells from turning around and following the wave. However, it has been demonstrated in several experiments that Dd cells are able to distinguish between temporarily rising or decreasing concentrations of the chemoattractant (see for instance Wessels *et al.* [49] or Geiger *et al.* [14]). Hence, we shall look at a kinetic model for chemotaxis that takes into account the ability of cells to react to temporal changes in the chemoattractant concentration. We shall see that in the limit this leads to a Keller-Segel model where the chemotactic sensitivity depends on the temporal derivative of the chemoattractant concentration.

2. A modelling framework

In the following, we consider cells moving on a surface or in three-dimensional space, and characterize the state of an individual cell by stochastic processes: its position $x(t) \in \Omega \subseteq \mathbb{R}^n$, its velocity $v(t) \in V \subseteq \mathbb{R}^n$, and some internal state $\zeta(t) \in Z \subseteq \mathbb{R}^k$, where $n = 2$ or 3, $k \in \mathbb{N}$ and time $t > 0$. The components of ζ are for instance concentrations of chemicals inside the cell or quantifications of other cell properties. We assume that inside every cell, $\zeta(t)$ evolves according to

$$\dot{\zeta} = \eta(x, \zeta, t) \ , \quad \zeta(t = 0) = \zeta_0 \tag{3}$$

Usually, the dependence of η on x and t will not be explicit but through external fields $S_i(x, t)$, $i = 1, .., N$ or their position gradients $\nabla S_i(x, t)$. Depending on the kind of external stimulus, these fields can be temperature, light, the electric field or, in the cases considered here, concentrations of chemoattractants. Then these fields are typically described by reaction-diffusion equations,

$$\delta_i \frac{\partial S_i}{\partial t} = \Delta S_i + g_i(S_1, ..., S_N, \rho). \tag{4}$$

Here, the functions g_i describe the reaction of S_i with the other chemicals and its production or consumption by the cells, whose total number density is given by

$$\rho(x, t) = \int_Z p(x, \zeta, t) d\zeta \, . \tag{5}$$

We shall discuss two stochastic mechanisms for the description of individual cell movement. If the cell's movement is driven by drift and by a *Brownian motion*, we

can describe the cell path by the stochastic differential equation (SDE)

$$dx = u_c(x,\zeta,t)dt + \sigma(x,\zeta)dB\ , \quad x(t=0) = x_0 \tag{6}$$

where $\sigma(x,\zeta)^2$ is the variance, u_c is the (chemotactic) drift velocity of the cell and $dB = dB(t,\omega)$ is the Brownian motion in $\mathbb{R}^n$. We shall assume for the following that η, u_c and σ are deterministic functions independent of the random variable ω. Associated to the SDE (3), (6) there is a linear partial differential equation, the *Fokker-Planck equation* for the phase space density $p(x,\zeta,t)$,

$$\frac{\partial p}{\partial t} + \nabla_x \cdot (pu_c) + \nabla_\zeta \cdot (p\eta) = \nabla_x \cdot (D\nabla_x p), \tag{7}$$

$$p(t=0) = p^{\mathrm{I}} \leq 0\ , \tag{8}$$

where the diffusion coefficient D is given by $D = \frac{\sigma^2}{2}$. With the initial condition $p^{\mathrm{I}} = \delta_{x_0,\zeta_0}$ the function $p(x,\zeta,t)$ for any time t can be interpreted as the probability density of a single cell. It can also be regarded as the density of an ensemble of cells starting from an initial density p^{I}. Here we adhere to the second interpretation and point out that birth and death processes have been neglected. We shall always consider boundary conditions such that the total number of cells

$$M = \int_{Z\times\Omega} p(x,\zeta,t)d\zeta dx \tag{9}$$

is constant in time, an assumption that is justified in the examples we are going to investigate later. Also, all the equations presented in this paper are already non-dimensionalized, and the number of parameters is reduced as far as possible. Note that no diffusion in the ζ-directions occurs in (7) due to the fact that we did not include a Brownian motion term in the state equation (3) for the internal variables.

Stochastic models for the motion of single cells and their connection to cell population models have been studied frequently in the literature. Dickinson and Tranquillo [8] present a general set of SDEs which govern the time evolution of the spatial distribution of bound and free receptors and the orientation and position of the cell. The authors use the so-called adiabatic elimination of fast variables to derive corresponding Fokker-Planck equations. This approach is used to describe chemotaxis and haptotaxis (taxis towards greater concentrations of adhesion molecules), see also [9]. In [45], the Keller-Segel model for chemotaxis is rigorously derived from an interacting stochastic many-particle system, where the interaction between the particles is rescaled in a moderate way as the population size tends to infinity. Ionides *et al.* [24] derive SDE models for the velocity of cells, and compare model predictions to data from experiments with human skin cells migrating in electric fields. Model parameters are estimated by using sequential Monte Carlo methods. A macroscopic model for the swarming of ants is derived rigorously from a stochastic process in Morale *et al.* [27].

The second class of stochastic models for cell movement are so-called *velocity-jump models*, where it is assumed that a cell moves with constant velocity in a straight line, stops after a certain time, chooses a new direction, continues running and so on. The generic example for this type of movement is the erratic motion ("run and tumble") of bacteria like *E. coli*. Typically, the tumbling time intervals are much shorter than the running periods, and it can be assumed that the turning events (and thus, changes of the cell's velocity v), are governed by a Poisson process.

The cell's position changes subject to

$$dx = v\,dt\,, \tag{10}$$

and new velocities are chosen after stochastically determined run times according to a probability distribution on V that can depend on the cell's previous or future velocity, its position x and its internal state ζ. The phase space density $P(x, v, \zeta, t)$ (now on the larger state space also including velocity v) satisfies the *Master equation* (*kinetic transport equation* in the context of gas dynamics or solid state/plasma physics)

$$\frac{\partial P}{\partial t} + v \cdot \nabla_x P + \nabla_\zeta \cdot (P\eta) = Q(P), \tag{11}$$

where the turning operator $Q(P)$ is defined by

$$Q(P) := \int_V \big[T(v' \to v, x, \zeta, t)P' - T(v \to v', x, \zeta, t)P\big]dv', \tag{12}$$

with $P' = P(x, v', \zeta, t)$. The turning kernel $T(v' \to v, x, \zeta, t) > 0$ describes velocity changes from v' to v, and usually depends on position x and time t through the external fields S_i or ∇S_i.

Equations (7) and (11) are posed on $(n+k)$- and, respectively, $(2n+k)$-dimensional phase spaces. In most situations, this complexity is prohibitive for numerical simulations, and most of the details contained in the solutions is not required. In the following, two typical simplification steps will be outlined, leading to dimension reductions. The first observation is that (7) and (11) are closely connected: If the turning operator in (11) satisfies certain assumptions specified below, then (7) can be derived as a scaling limit of (11), replacing $2n$ by n in the dimensionality of the description. A second simplification step will replace the $(n + k)$-dimensional equation (7) by $k+1$ equations on the n-dimensional position space. The possibility to carry out the two simplifications in different orders leads to 4 steps described in the 4 paragraphs below.

Macroscopic limit 1. Key requirement for the passage from (11) to (7) is that the turning processes are predominantly without directional bias. We assume that the turning operator $Q(P)$ in (12) can be written as

$$Q(P) = Q_0(P) + \varepsilon Q_1(P)\,,$$

where ε is a small, dimensionless parameter representing the ratio between biased and nonbiased contributions to the turning process. We require that the leading order turning operator $Q_0(P)$ has a one-dimensional kernel (fixing x, ζ and t) such that

$$Q_0(P) = 0 \Leftrightarrow P(x, v, \zeta, t) = p(x, \zeta, t)F(v; x, \zeta, t), \tag{13}$$

where the normalized *equilibrium distribution* F satisfies

$$\int_V F\,dv = 1 \quad \text{and} \quad \int_V vF\,dv = 0. \tag{14}$$

The second relation states that the mean flux of the limit equilibrium distribution vanishes, i.e., that the leading order turning processes describe undirected motion of cells. As a consequence, when introducing macroscopic variables, a parabolic

scaling, $x \to x/\varepsilon$ and $t \to t/\varepsilon^2$, of space and time is appropriate. Additionally, we rescale $\eta \to \varepsilon^2\eta$. Thus, equation (11) becomes

$$\varepsilon^2 \frac{\partial P}{\partial t} + \varepsilon v \cdot \nabla_x P + \varepsilon^2 \nabla_\zeta \cdot (P\eta) = Q_0(P) + \varepsilon Q_1(P). \tag{15}$$

Defining the functions

$$R = \frac{P - pF}{\varepsilon}, \text{ where } p(x,\zeta,t) = \int_V P(x,v,\zeta,t)\, dv \tag{16}$$

and dividing by ε, we can write equation (15) as

$$\varepsilon \frac{\partial P}{\partial t} + v \cdot \nabla_x P + \varepsilon \nabla_\zeta \cdot (P\eta) - Q_1(P) = Q_0(R). \tag{17}$$

In the (formal) limit $\varepsilon \to 0$, it follows from (15) that $Q_0(P_0) = 0$. As a consequence of (13), this means that $P \to P_0 = p_0 F$. Denoting $R_0 := \lim_{\varepsilon\to 0} R$ and letting $\varepsilon \to 0$ in (17), we deduce

$$Q_0(R_0) = vF \cdot \nabla_x p_0 + (v \cdot \nabla_x F - Q_1(F))\, p_0. \tag{18}$$

Now we integrate (15) with respect to v and divide by ε^2:

$$\frac{\partial p}{\partial t} + \nabla_x \cdot \int_V vR\, dv + \nabla_\zeta \cdot (p\eta) = 0, \tag{19}$$

where we used the fact that, due to $\int Q(P)dv = 0$, conservation of the total number of cells is a property of the model. As $\varepsilon \to 0$, we obtain

$$\frac{\partial p_0}{\partial t} + \nabla_x \cdot \int_V vR_0 dv + \nabla_\zeta \cdot (p_0\eta) = 0. \tag{20}$$

From (18), it follows that the function R_0 can be written as

$$R_0 = \Gamma \cdot \nabla_x p_0 + \gamma p_0, \tag{21}$$

where

$$Q_0(\Gamma) = vF \text{ and } Q_0(\gamma) = v \cdot \nabla_x F - Q_1(F). \tag{22}$$

Note that R_0 is not uniquely determined, as we can always add a function which is in the kernel of Q_0. However, the second term in (20) is not influenced by this fact, and we obtain

$$\int_V vR_0 dv = -D\nabla_x p_0 + u_c p_0,$$

with

$$D = -\int_V v \otimes \Gamma dv \text{ and } u_c = \int_V v\gamma dv. \tag{23}$$

As a consequence, we can write (20) as

$$\frac{\partial p_0}{\partial t} + \nabla_x \cdot (p_0 u_c) + \nabla_\zeta \cdot (p_0\eta) = \nabla_x \cdot (D\nabla_x p_0), \tag{24}$$

which is exactly the Fokker-Planck equation (7).

Note that the solvability of the inhomogeneous equations (22) is crucial for a rigorous justification of the limit process ML1 in figure 1.

Remark 1. *If assumption (14) is not satisfied (which means that directed instead of random movement is dominating), the correct scaling is hyperbolic, i.e.* $x \to x/\varepsilon$ *and* $t \to t/\varepsilon$*, and* $\eta \to \varepsilon\eta$*. Performing the corresponding macroscopic limit then leads to a convection equation for* p_0*,*

$$\frac{\partial p_0}{\partial t} + \nabla_x \cdot (p_0 u_c) + \nabla_\zeta \cdot (p_0 \eta) = 0, \tag{25}$$

where the chemotactic velocity u_c *is now given by*

$$u_c = \int_V vF\, dv. \tag{26}$$

Moment expansion 1. The second simplification step is of a more heuristic nature using certain *ad hoc* assumptions. We start with the Fokker-Planck equation (7) and aim for a model in terms of the position density of cells and of the average values of the internal quantities,

$$\rho(x,t) = \int_Z p(x,\zeta,t)d\zeta\,, \qquad (\rho z)(x,t) = \int_Z \zeta\, p(x,\zeta,t)d\zeta\,. \tag{27}$$

Integration of (7) with respect to ζ gives

$$\frac{\partial \rho}{\partial t} + \nabla_x \cdot \int_Z p u_c d\zeta = \nabla_x \cdot \int_Z D\nabla_x p\, d\zeta, \tag{28}$$

where we used the biologically reasonable boundary condition $(p\eta)(x,\zeta,t) = 0$ for $\zeta \in \partial Z$. On the other hand, multiplying (7) by ζ and integrating again gives

$$\frac{\partial (\rho z)}{\partial t} + \nabla_x \cdot \int_Z p\zeta u_c d\zeta - \int_Z p\eta d\zeta = \nabla_x \cdot \int_Z D\nabla_x (p\zeta) d\zeta. \tag{29}$$

In order to to write the equations (28) and (29) in a self-consistent way, we have to make closure assumptions for the fluxes and for the reaction terms. These are by no means unique, and instead of the *ad hoc* choices proposed here, evidence from experiments and/or numerical simulations on the distributions of the internal variables might be used. An example is contained in Section 5.

A simple way to achieve closure is to replace the internal variable ζ by its mean value z in the drift velocity u_c, in the diffusivity D, and in the reaction term η in all the integrals in (28) and (29). This leads to the fluid type equations in position space

$$\frac{\partial \rho}{\partial t} + \nabla_x \cdot (\rho u_c) = \nabla_x \cdot (D\nabla_x \rho) \tag{30}$$

and

$$\frac{\partial (\rho z)}{\partial t} + \nabla_x \cdot (\rho z u_c) = \nabla_x \cdot (D\nabla_x (\rho z)) + \rho\eta, \tag{31}$$

where D, u_c and η are evaluated at $\zeta = z$. If the chemotactic velocity is of the form $u_c = \chi(\rho, S)\nabla S$ (independent of z), equation (30) becomes equation (1) of the Keller-Segel model.

Moment expansion 2. The simplification steps might also be carried out in reverse order to produce the commuting diagram of Figure 1.

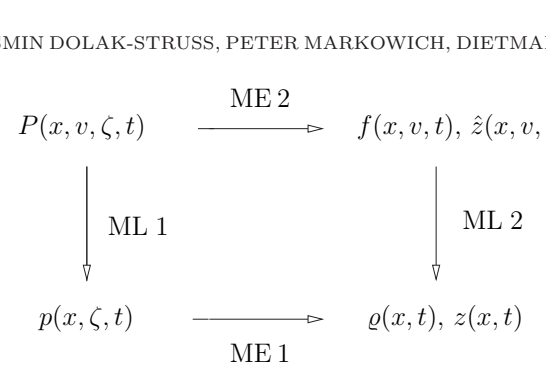

FIGURE 1

We start again with the full master equation (11) for the velocity jump model and try to obtain a model in terms of the position-velocity space density of cells and the position-velocity dependent mean values of internal quantities,

$$f(x,v,t) = \int_Z P(x,v,\zeta,t)\,d\zeta, \qquad (\hat{z}f)(x,v,t) = \int_Z \zeta\, P(x,v,\zeta,t)\,d\zeta\,. \tag{32}$$

We proceed as before: integration of (11) with respect to ζ yields

$$\frac{\partial f}{\partial t} + v\cdot\nabla_x f = \int_Z Q(P)d\zeta, \tag{33}$$

whereas multiplication of (11) by ζ and integration gives

$$\frac{\partial(\hat{z}f)}{\partial t} + v\cdot\nabla_x(\hat{z}f) - \int_Z P\eta d\zeta = \int_Z Q(\zeta P)d\zeta. \tag{34}$$

Keeping in mind that $Q(P)$ is defined by (12), we approximate the right hand side of (33) by $\bar{Q}(f)$, where

$$\bar{Q}(f) = \int_V \big[T(v'\to v,x,\hat{z}(x,v'),t)f' - T(v\to v',x,\hat{z}(x,v),t)f\big]dv', \tag{35}$$

and the right hand side of (34) by $\bar{Q}(\hat{z}f)$. Note that we replaced the internal variable in the turning rate by its mean value at the velocity before turning. As in (31), we finally approximate

$$\int_Z P(x,v,\zeta)\eta(x,\zeta)d\zeta \sim f(x,v)\eta(x,\hat{z}(x,v)) \tag{36}$$

to obtain from (33), (34) the closed model

$$\frac{\partial f}{\partial t} + v\cdot\nabla_x f = \bar{Q}(f) \tag{37}$$

and

$$\frac{\partial(\hat{z}f)}{\partial t} + v\cdot\nabla_x(\hat{z}f) - f\eta = \bar{Q}(\hat{z}f). \tag{38}$$

Equation (37) is a kinetic transport equation sharing the left hand side with the Boltzmann equation of gas dynamics. In the context of chemotaxis, an equation of type (37) (without internal dynamics) was first derived from a velocity jump process by Stroock [46] in 1974. Othmer *et al.* [30] discussed position and velocity jump models for various biological applications and investigated the corresponding macroscopic equations.

Macroscopic limit 2. To complete the commuting diagram in Fig. 1, we will now investigate the macroscopic limit of system (37), (38). Obtaining a drift-diffusion equation as macroscopic limit of an kinetic equation like (37) has been investigated by several authors, for a detailed discussion of appropriate approaches to this problem see Section 3. We now assume that $\bar{Q}(f)$ can be written as $\bar{Q}_0(f) + \varepsilon\bar{Q}_1(f)$, where for every velocity independent $\hat{z}(x,v,t) = z(x,t)$, $\bar{Q}_0$ has a one-dimensional kernel:

$$\bar{Q}_0(f) = 0 \Leftrightarrow f(x,v,t) = \rho(x,t)\bar{F}(v;x,z(x,t),t)\,,$$

satisfying (14). As before, we rescale space and time (diffusion scaling) as well as the function η, to obtain

$$\varepsilon^2\frac{\partial f}{\partial t} + \varepsilon v\cdot\nabla_x f = \bar{Q}_0(f) + \varepsilon\bar{Q}_1(f) \tag{39}$$

$$\varepsilon^2\frac{\partial(\hat{z}f)}{\partial t} + \varepsilon v\cdot\nabla_x(\hat{z}f) - \varepsilon^2 f\eta = \bar{Q}_0(\hat{z}f) + \varepsilon\bar{Q}_1(\hat{z}f). \tag{40}$$

The limiting equations $\bar{Q}_0(f_0) = \bar{Q}_0(\hat{z}_0 f_0) = 0$ as $\varepsilon \to 0$ then have solutions $f_0(x,v,t) = \rho_0(x,t)\bar{F}(v;x,z_0(x,t),t)$, $(\hat{z}_0 f_0)(x,v,t) = \rho_0(x,t)z_0(x,t)\bar{F}(v;x,z_0(x,t),t)$. Following the procedure introduced in the last section, we obtain the macroscopic equations

$$\frac{\partial\rho_0}{\partial t} + \nabla_x\cdot(\rho_0\, u_c) = \nabla_x\cdot(D\nabla_x\rho_0) \tag{41}$$

$$\frac{\partial(\rho_0 z_0)}{\partial t} + \nabla_x\cdot(\rho_0 z_0 u_c) = \nabla_x\cdot(D\nabla_x(\rho_0 z_0)) + \rho_0\eta. \tag{42}$$

The chemotactic velocity u_c and the diffusion coefficient D are again given by (23) (but, like γ and Γ, depending on z_0 now). Note that system (41-42) is exactly the same as (30-31).

The two paths from the master equation (11) to the fluid model (30-31) visit two different intermediate models: the Fokker-Planck equation (7), which will be the starting point of the leukocyte modelling in Section 5, and the kinetic model (37-38), which is at the basis of the Dd model of Section 6.

3. Rigorous macroscopic limits of kinetic models

This section contains rigorous justifications of the 'macroscopic limit 2' (ML2 in Figure 1). We shall restrict our attention to situations without internal variables and consider the convergence of solutions of the kinetic equation (37) to solutions of a Keller-Segel type model (whose parameters can be directly computed from the turning kernel T) when ε tends to zero. We shall present two results: one on the diffusive and one on the purely convective limit (see Remark 1 above).

The proof of the main theorem on the diffusive limit is spread in different references (see [4, 22, 5]), and here we only show its main features and omit technical details.

To fix notation, we consider

$$\varepsilon^2\frac{\partial f_\varepsilon}{\partial t} + \varepsilon v\cdot\nabla_x f_\varepsilon = Q_\varepsilon[S_\varepsilon,\rho_\varepsilon]f_\varepsilon\,, \quad x\in\mathbb{R}^n,\ v\in V,\ t>0, \tag{43}$$

$$f_\varepsilon(t=0) = f^{\mathrm{I}}\,, \tag{44}$$

with the *turning operator*

$$Q_\varepsilon[S_\varepsilon,\rho_\varepsilon]f(v)=\int_V \left(T_\varepsilon(v'\to v)[S_\varepsilon,\rho_\varepsilon]f(v')-T_\varepsilon(v\to v')[S_\varepsilon,\rho_\varepsilon]f(v)\right)dv' \tag{45}$$

depending on a chemoattractant density S_ε and the macroscopic cell density ρ_ε. The chemoattractant density solves a quasistationary approximation of the reaction diffusion equation (2) with a simple model for production of the chemoattractant by the cells, namely the Poisson equation

$$-\Delta S_\varepsilon=\rho_\varepsilon:=\int_V f_\varepsilon dv\,,\quad x\in\mathbb{R}^n,\ t>0. \tag{46}$$

We impose the following assumptions on the turning kernel:
When $S_\varepsilon\to S_0$ and $\rho_\varepsilon\to\rho_0$ as $\varepsilon\to 0$, then

$$T_\varepsilon(v\to v')[S_\varepsilon,\rho_\varepsilon]=T_0(v\to v')[S_0,\rho_0]+\varepsilon T_1(v\to v')[S_0,\rho_0]+o(\varepsilon)$$

where the convergence $T_\varepsilon\to T_0$ is made precise in reference [4].
There exists a velocity distribution $0<F(v)\in L^\infty(V)$, independent of x, t, S and ρ such that the detailed balance equation $T_0(v'\to v)[S,\rho]F(v)=T_0(v\to v')[S,\rho]F(v')$ and the properties (14) hold. The turning rate $T_0[S,\rho]$ is bounded and there exists a constant $\gamma>0$ such that $T_0[S,\rho]/F\geq\gamma$, $\forall(v,v')\in V\times V$, $x\in\mathbb{R}^n$, $t>0$.

Let the initial condition be given by

$$f^{\mathrm{I}}(x,v)=\rho^{\mathrm{I}}(x)F(v)\in L^1_+(\mathbb{R}^n\times V)\cap L^p\left(\mathbb{R}^n\times V,\frac{dx\,dv}{F^{p-1}}\right)\,,$$

for a $p>n$. Let us also suppose that

$$\begin{aligned}\phi^S_\varepsilon[S,\rho] &\geq \gamma(1-\varepsilon\Lambda(||S||_{W^{1,\infty}}))FF'\,,\\ \int_V\frac{\phi^A_\varepsilon[S,\rho]^2}{F\phi^S_\varepsilon[S,\rho]}dv' &\leq \varepsilon^2\Lambda(||S||_{W^{1,\infty}})\,,\end{aligned}$$

where

$$\begin{aligned}\phi^S_\varepsilon &:= \frac{T_\varepsilon(v\to v')[S,\rho]F(v')+T_\varepsilon(v'\to v)[S,\rho]F(v)}{2}\,,\\ \phi^A_\varepsilon &:= \frac{T_\varepsilon(v\to v')[S,\rho]F(v')-T_\varepsilon(v'\to v)[S,\rho]F(v)}{2}\,.\end{aligned}$$

Then, there is $t^*>0$, independent of ε, such that

$$\begin{aligned}\rho_\varepsilon &\to \rho_0 \ \text{ in } L^2_{\mathrm{loc}}(\mathbb{R}^n\times(0,t^*))\,,\\ S_\varepsilon &\to S_0 \ \text{ in } L^q_{\mathrm{loc}}(\mathbb{R}^n\times(0,t^*))\,,1\leq q<\infty\,,\\ \nabla S_\varepsilon &\to \nabla S_0 \ \text{ in } L^q_{\mathrm{loc}}(\mathbb{R}^n\times(0,t^*))\,,1\leq q<\infty.\end{aligned}$$

Here ρ_0 and S_0 denote the time-local solution of the Keller-Segel model

$$\begin{aligned}\frac{\partial\rho_0}{\partial t}+\nabla\cdot(\chi[\rho_0,S_0]\rho_0) &= \nabla\cdot(D_\rho(\rho_0,S_0)\nabla\rho_0)\\ -\Delta S_0 &= \rho_0\,.\end{aligned}$$

where $\chi[\rho_0,S_0]$ and $D_\rho(\rho_0,S_0)$ are given by

$$\begin{aligned}\chi[\rho_0,S_0] &= -\int_V v\,\Theta[S_0,\rho_0](x,v,t)\,dv\,,\ \text{with}\quad Q_0[S_0,\rho_0](\Theta)=Q_1[S_0,\rho_0](F)\\ D_\rho(\rho_0,S_0) &= -\int_V v\otimes\kappa[S_0,\rho_0](x,v,t)\,dv\,,\ \text{with}\quad Q_0[S_0,\rho_0](\kappa)=vF\,.\end{aligned}$$

For an appropriate choice of the turning kernel we may obtain the classical Keller Segel model with constant χ and D_ρ (see [4]).

Proof. (Sketch) After having performed the formal limiting procedure in the previous section we prove local in time, uniform in ε a priori bounds (i.e., the existence of a ε-independent time t^* such that):

$$f_\varepsilon \in L^\infty\left(0,t^*;\mathcal{X}_p\right)\ ,\ \mathcal{X}_p = L^\infty\left(0,t^*;L^1_+(\mathbb{R}^n\times V)\cap L^p\left(\mathbb{R}^n\times V,\frac{dx\,dv}{F^{p-1}}\right)\right)$$

$$S_\varepsilon \in L^\infty\left(0,t^*;W^{1,q}(\mathbb{R}^n)\cap C^{1+\alpha}(\mathbb{R}^n)\right)\ ,\ 1\le q<\infty\ ,\ 0<\alpha<\frac{p-n}{p}\ ,$$

$$r_\varepsilon := \frac{f_\varepsilon-\rho_\varepsilon F}{\varepsilon}\in L^2\left(\mathbb{R}^n\times V\times[0,t^*);\frac{dx\,dv\,dt}{F}\right).$$

The next step consists in proving the strong convergence of S_ε and ∇S_ε. For this we prove compactness in position and time using results from potential theory (particularly from elliptic regularity) and the uniform a priori bounds. The last part consists in proving the strong convergence of ρ_ε, which follows from compensated compactness. □

Examples of turning kernels, which satisfy assumptions of the previous theorem, can be found in the references [4, 22, 23, 5, 6]. Generalizations of Theorem 1 allow for more general (parabolic) models for the chemoattractant dynamics [22, 23].

Memory effects have been taken into account in [10] in a kinetic model satisfying the following assumptions.
The turning kernel $T:\mathbb{R}_+\times\mathbb{R}\to\mathbb{R}_+$ depends on the local value of the chemoattractant concentration S as well as on its time derivative along an incoming path, i.e. $T[S](v'\to v,x,t)=T(S(x,t),S_t(x,t)+v'\cdot\nabla S(x,t))$.
T is smooth, monotonically decreasing in its second argument and satisfies

$$0<\alpha\le T\le\beta, \tag{47}$$

with positive constants α and β. The null space of a turning operator $Q[S]$ with these assumptions is spanned by

$$F(v;x,t)=\frac{T_0(x,t)}{T(S(x,t),S_t(x,t)+v\cdot\nabla S(x,t))}\ ,\quad \frac{1}{T_0}=\int_V\frac{dv'}{T(S,S_t+v'\cdot\nabla S)}\ ,$$

satisfying $F>0$ and $\int_V F\,dv=1$, but the mean velocity

$$u_c=\int_V vF\,dv=\chi(S,S_t,|\nabla S|)\nabla S,\quad \chi(S,S_t,|\nabla S|)=\frac{T_0}{|\nabla S|}\int_V\frac{v_1dv}{T(S,S_t+v_1|\nabla S|)} \tag{48}$$

does not vanish in general.

In contrast to the parabolic scaling used above, a *hydrodynamic scaling* is now appropriate:

$$\varepsilon\frac{\partial f_\varepsilon}{\partial t}+\varepsilon v\cdot\nabla_x f_\varepsilon = Q[S]f_\varepsilon\ , \tag{49}$$

$$f_\varepsilon(t=0)=f^{\mathrm{I}} \tag{50}$$

For the macroscopic limit $\varepsilon\to 0$, the following convergence result holds: Let the initial condition be well prepared, i.e.

$$f^{\mathrm{I}}(x,v)=\rho^{\mathrm{I}}(x)F^{\mathrm{I}}(v;x),\quad \text{with}\quad Q\big|_{t=0}(F^I)=0.$$

Furthermore, assume that $f^{\mathrm{I}}(x,v)$ is smooth and $f^{\mathrm{I}}(x,v)=0$ for $x\notin K$, K compact, and that $S(x,t)$ is a smooth, given function. Let f_ε be the solution of problem (49), (50) for $t<t^*$. Then,

$$f_\varepsilon \to \rho_0 F \ \text{ in } L^\infty_{\mathrm{loc}}((0,t^*),L^1(\mathbb{R}^n\times V)),$$

and there exists a positive constant C_{t^*} depending on the data such that

$$\sup_{0<t<t^*}\|f_\varepsilon-\rho_0 F\|_{L^1(\mathbb{R}^n\times V)}\le C_{t^*}\varepsilon.$$

Here, ρ_0 is the solution of (41) for $t<t^*$, with $D_0\equiv 0$ and the chemotactic velocity is given by (48).

Proof. Using the Hilbert expansion for f_ε, i.e, $f_\varepsilon=f_0+\varepsilon f_1+\dots$, the proof is based on an estimate of the remainder $r_\varepsilon=f_\varepsilon-(f_0+\varepsilon f_1)$ solving a problem of the form (49) with vanishing initial data and an $O(\varepsilon^2)$-inhomogeneity in the transport equation. The non-negativity of the chemotactic sensitivity χ in the limiting equation is a consequence of the assumption that T is decreasing in its second argument. □

Remark 2. *The estimation of the remainder r_ε is based on similar arguments as in* [43]. *In* [10]*, more general initial conditions are considered (i.e., $Q(f^I)=0$ is not assumed to hold), which leads to an initial layer problem.*

The above proof relies on the Hilbert expansion of f_ε to derive the limiting equations. An alternative approach for obtaining correction terms is the so-called *Chapman-Enskog expansion*, based on the micro-macro-decomposition

$$f_\varepsilon(x,v,t)=\rho_\varepsilon(x,t)F(v;x,t)+\varepsilon f_\varepsilon^\perp(x,v,t),\quad \int_V f_\varepsilon^\perp\,dv=0\,. \tag{51}$$

By applying the corresponding projections to the kinetic equation (49) leads to a system for the new unknowns ρ_ε and $f_\varepsilon^\perp$. The Chapman-Enskog expansion now consists in computing approximations for an equation for the macroscopic variable ρ_ε after elimination of the microscopic variable $f_\varepsilon^\perp$. At leading order, the purely convective limit equation of the above theorem is obtained. The $O(\varepsilon)$-correction, however, provides a diffusion term (see also section 6). For details, we refer the reader to [10].

4. Global existence and blow up for models of chemotaxis

In this section we state some results on global existence and local in time blow up, mostly without proofs. Complete proofs can be found in the references.

For the classical Keller-Segel model with chemoattractant production by the cells, the behaviour strongly depends on the space dimension. Generically, blow up in finite time does not occur in 1D and always occurs in 3D. Here we shall shortly discuss the situation in 2D which is characterized by a threshold phenomenon. We also consider several regularizations leading to global existence. We concentrate on simple models of the form

$$\frac{\partial\rho}{\partial t}+\nabla_x\cdot(\rho u_c[\rho,S]) = \nabla_x\cdot(D_0\nabla_x\rho)\ , \tag{52}$$

$$-\Delta S = \rho\ . \tag{53}$$

with $\rho(x,0)=\rho^{\mathrm{I}}(x)\ge 0$, and decay conditions for S in the limit $|x|\to\infty$. We define the constant *total mass* $M:=\int_{\mathbb{R}^n}\rho^{\mathrm{I}}dx$. D_0 is a positive constant and $\chi(\rho)>0$.

Blow up and global existence have been studied for many particular cases. We refer to [16, 15, 28, 29] and references therein. We collect four global existence results: For $n = 2$, if one of the conditions below is satisfied:
Subcritical total mass[12]: $u_c = \chi_0 \nabla S$ with $\chi_0 > 0$ and $M < 8\pi D_0/\chi_0$, or
Quorum sensing 1[18]: $u_c = \chi(\rho)\nabla S$ and there is a threshold $\bar\rho > 0$ such that $\chi(\rho) = 0$ for $\rho \geq \bar\rho$ or, more generally,
Quorum sensing 2[48]: $\chi(\rho) \to 0$ sufficiently fast as $\rho \to \infty$, or
Finite sampling radius[19]: $u_c = \chi_0 \overset{\circ}{\nabla}_\rho S$ with $\overset{\circ}{\nabla}_\rho S(x) = \frac{1}{\pi R}\int_{|\omega|=1} \omega S(x + R\omega)d\omega$, $R > 0$, then the model (52–53) has global weak solutions.

The threshold given in the first result has recently been proven to be sharp: [12] For $n = 2$, $\chi(\rho) \equiv \chi_0 > 0$, $M := \int_{\mathbb{R}^2} \rho^{\mathrm{I}} dx < \infty$, if $M > 8\pi D_0/\chi_0$, then solutions of the Keller-Segel model (52–53) blow up in finite time.

Proof. We present the proof of Theorem 4 here since it conveys significant insight into the dynamics of the Keller-Segel model. We solve Equation (53):

$$S(x,t) = -\frac{1}{2\pi}\int_{\mathbb{R}^2} \log|x-y|\rho(y,t)dy \ ,$$

then, multiply Equation (52) by $|x|^2$ and integrate by parts. We find

$$\frac{1}{2}\frac{d}{dt}\int_{\mathbb{R}^2} |x|^2\rho dx = 2D_0 M + \chi_0 \int_{\mathbb{R}^2} \rho\nabla S \cdot x dx \ .$$

We also have

$$\int_{\mathbb{R}^2} \rho\nabla S\cdot x dx = -\frac{1}{2\pi}\int_{\mathbb{R}^2\times\mathbb{R}^2} \rho(x,t)\rho(y,t)\frac{x-y}{|x-y|^2}\cdot x dx\, dy =$$
$$\text{(exchanging } x \text{ and } y!) \quad = -\frac{1}{4\pi}\int_{\mathbb{R}^2\times\mathbb{R}^2} \rho(x,t)\rho(y,t)dx\, dy = -\frac{M^2}{4\pi} \ .$$

Finally,

$$\frac{1}{2}\frac{d}{dt}\int_{\mathbb{R}^2} |x|^2\rho(x,t)dx = 2M\left(D_0 - \frac{\chi_0}{8\pi}M\right) \ .$$

If $M > 8\pi D_0/\chi_0$, then $\int_{\mathbb{R}^2}\rho(x,t)dx$ becomes 0 in finite time which implies $\rho(x,t_0) = \delta(x)$ for some $t_0 \in (0,\infty)$. □

Remark 3. *The difficulty in the issue of global existence is that the production of the chemoattractant by the cells produces an attractive force, just as in models for gravitational interaction of particles. This is completely different from the situation when the chemoattractant is consumed by the cells and (53) has to be replaced by $+\Delta S = \rho$. This creates a repulsive interaction, just as in models for charged particles (compare, e.g., to the drift-diffusion system of semiconductors* [26]*). In the latter case time-global smooth solutions are know to exist* [7].

We outline a proof. Consider a function $\mathcal{F}(s)$ such that $\mathcal{F}''(s) \geq 0$, $\mathcal{F}'' \not\equiv 0$ and set

$$\mathcal{G}(s) := \int_0^s s'\mathcal{F}''(s')ds' \ .$$

Then, we multiply (52) by $\mathcal{F}'(s)$ and integrate by parts:

$$\frac{d}{dt}\int_{\mathbb{R}^n}\mathcal{F}(\rho)dx = -D_0\int_{\mathbb{R}^n}|\nabla\rho|^2\mathcal{F}(\rho)dx + \chi_0\int_{\mathbb{R}^n}\rho\mathcal{F}''(\rho)\nabla\rho\cdot\nabla S dx = \\ = -D_0\int_{\mathbb{R}^n}|\nabla\rho|^2\mathcal{F}''(\rho)dx - \chi_0\int_{\mathbb{R}^n}\rho\mathcal{G}(\rho)dx \leq 0\ .$$

Finally, if we chose $\mathcal{F}(s) = s^\alpha$ with $\alpha > 1$, we immediately conclude the existence of a global bound for the $L^\alpha(\mathbb{R}^n)$-norm, i.e., there is no concentration of mass in ρ.

Recently, global existence for certain kinetic models has been proven. We shall state to typical results.

[4] If the turning kernel is such that

$$0 \leq T(v'\to v)[S,\rho] \leq C(1 + S(x+v,t) + S(x-v,t))\ , \tag{54}$$

then there exists a global solution (f, S) of the kinetic model (43–46).

Remark 4. *It is possible to devise a kinetic model for chemotaxis with global existence of solutions such that the solutions of its drift-diffusion limit blow up in finite time. For a turning kernel given by*

$$T(v'\to v)[S,\rho] = \Psi(S(x+v,t) - S(x,t))$$

with Ψ at most linear, Theorem 4 applies and its associated macroscopic limit is the classical (i.e., with constant coefficients D_0 and χ_0) Keller-Segel model. For details, see [4].

For kinetic models such that the chemotactical part $T_\varepsilon - T_0$ of the turning kernel vanishes if the cell density becomes sufficiently large, as, for example

$$T_\varepsilon(v'\to v)[S,\rho] = \lambda(x,t)F(v) + \varepsilon a(\rho,S)F(v)v\cdot\nabla S\ , \\ \text{with } a(\rho,S) = 0 \text{ if } \rho \geq \bar\rho\ , \text{or} \tag{55}$$

$$T_\varepsilon(v'\to v)[S,\rho] = \psi(S(x,t), S(x+\varepsilon\mu(\rho)v,t)\ , \\ \text{with } \mu(\rho) = 0\ ,\ \text{if } \rho \geq \bar\rho\ , \tag{56}$$

we have: [5] Consider the kinetic model for chemotaxis (43–46) with turning kernel given by (55) or (56). For ε small enough, its solution (f, S) exists globally. Furthermore

$$||\rho(\cdot,t)||_{L^\infty(\mathbb{R}^n)} \leq \max\{||\rho^{\mathrm{I}}||_{L^\infty(\mathbb{R}^n)}, \bar\rho\}\ . \tag{57}$$

The second result in Theorem 4 can now also be obtained as a corollary [5] of this theorem (together with theorem 3).

Models with prevention of blow up can be used for studying the dynamics of cell aggregates. The long-time behavior of the Keller-Segel model with $\chi = (1-\rho)$ coupled to a parabolic equation for S has been investigated for one space dimension in [42]. Dolak and Schmeiser [11] study a similar system with an elliptic equation for S and a small diffusion constant ε. These models show a very interesting long-time behavior: starting from almost homogeneous initial conditions, plateau-like patterns with the cell density varying between 1 and 0 emerge quickly, and seem to remain stationary for a long time. However, the smaller plateaus are attracted by the larger ones, and slowly move towards them. When a certain minimum distance between the plateaus has been reached, the smaller plateau collapses and merges

with the larger one. This coarsening process continues until only one plateau at one of the domain boundaries is left. The time it takes the plateaus to merge depends exponentially on the domain length [42] or, if the length remains fixed, on the inverse of the diffusion constant ε [11]. For the latter case, the authors derive an ODE system describing the movement of the plateau boundaries using the method of exponential asymptotics, based on a linearization around an approximate steady state.

5. A stochastic model with memory effects for multiple chemoattractants

In this section we review results from [38] and [39], concerned with the chemotactic movement of leukocytes in the presence of several different chemoattractants.

Let the cell position $x(t) \in \mathbb{R}^2$ and assume the presence of k chemoattractant substances with concentrations $S_i(x)$, $1 \le i \le k$, assumed stationary for simplicity.

Every single cell has receptors which let the cell perceive the directions and strengths of chemoattractant gradients. Motivated by experimental evidence[13] we assume that each cell has a dynamically changing sensitivity $\zeta_i(t) \ge 0$ for the chemoattractant S_i, $1 \le i \le k$. These represent the responsiveness of cells to the presence of the respective chemoattractant gradient which depends, among other things, on the absolute number of receptors for the respective chemoattractant and on the number of "free" receptors, i.e. on the fraction of receptors which are not bound to a chemoattractant molecule.

To obtain a formula for the chemotactic velocity, we therefore sum up the contributions $\zeta_i \nabla S_i$. Inclusion of random effects leads to a stochastic differential equation of type (6) for the evolution of the spatial position of a single leukocyte:

$$dx = u_c(x,\zeta)\, dt + \sigma\, dB, \qquad \text{with } u_c(x,\zeta) = \sum_{i=1}^{m} \zeta_i \nabla S_i(x)\,, \tag{58}$$

where the standard deviation $\sigma > 0$ is assumed constant.

Experimental evidence also indicates that the sensitivity for a chemoattractant is downregulated in situations where the concentration of this chemoattractant is high. For that reason we assume that for each sensitivity ζ_i the vector $S := (S_1, \dots, S_k)^T$ of chemoattractant concentrations is mapped to some target value in the interval $[\zeta_i^{\min}, \zeta_i^{\max}]$. The target values are given by

$$\hat{\zeta}_i(S) := \zeta_i^{\min} + \frac{1}{(AS)_i + (\zeta_i^{\max} - \zeta_i^{\min})^{-1}}, \quad i = 1, \dots, k, \tag{59}$$

where $A = (a_{ij})_{1 \le i,j \le k}$, $a_{ij} \ge 0$ is the matrix of downregulation factors. In the case where sensitivities are only downregulated by their associated chemoattractants, it is a diagonal matrix. Note that the expression (59) can be derived from discrete random walks (see [41]). Observe that $\zeta_i^{\min}$ and $\zeta_i^{\max}$ are those levels for the sensitivity which are reached when downregulation is maximal, respectively minimal.

Experiments show the ability of leukocytes to navigate from one chemoattractant source to the next. This would be impossible to describe with a standard Keller-Segel type model, where the sensitivities assume their target values instantaneously. The main feature of our model is the assumption that the sensitivities adapt to the

target values with a delay. Their dynamics is given by

$$d\zeta_i = \eta(x,\zeta) = \kappa_i(\hat{\zeta}_i(S(x)) - \zeta_i)dt, \tag{60}$$

where $\kappa_i > 0$ is the rate of adaption of the sensitivity ζ_i.

In [39] a dynamical systems analysis of a deterministic version (with $\sigma = 0$) of (58), (60) has been carried out for the special case $k = 2$ of two chemoattractants whose concentrations are stationary Gaussians. The system exhibits a supercritical Hopf bifurcation. The bifurcation parameter corresponds to a scaled version of the relaxation time of the sensitivities. For small values of this parameter, the system has a stable fixed point between the peaks, i.e. cells migrate to this position, whereas for slow sensitivity relaxation, the system has a stable limit cycle, i.e., cells keep moving back and forth between the two chemoattractant peaks, which is the desired behaviour.

Returning to the stochastic system (58), (60), parameter values are chosen corresponding to the latter situation described above. We expect the existence of a stable invariant measure and compare two numerical approaches for its computation.

On the one hand, the stochastic system is solved straightforwardly by a 'direct simulation Monte Carlo' method. The resulting steady state distribution $\rho(x)$ in position space is depicted in Figure 2(a).

The second approach starts with the Fokker-Planck equation (7) for the distribution function $p(x,\zeta,t)$ and performs a simplification as in *moment expansion 1* in Section 2. Observe that the set of possible sensitivity configurations is given by $Z := [\zeta_1^{\min},\zeta_1^{\max}] \times \ldots \times [\zeta_k^{\min},\zeta_k^{\max}]$ and define the macroscopic density ρ and the mean values z of the sensitivities by (27). It turns out that a closure assumption is only needed for the flux term in the z-equation. However, the simple closure used in Section 2 would be inappropriate here. It is important that at one point between the chemoattractant peaks cells with stronger sensitivity for one chemoattractant or the other may exists simultaneously. Therefore the essential dynamic behaviour would be destroyed by representing sensitivities only by their mean values. As a consequence, we expand the closure assumption (31) using a symmetric, positive definite covariance matrix $C = (c_{ij})_{k\times k}$ as an additional modelling parameter and introduce the closure

$$\int_Z p\zeta_i u_c d\zeta \sim \rho\left(z_i u_c(z) + \sum_{j=1}^{k} c_{ij}\nabla S_j\right) .$$

Then the system of moments (30), (31) reads

$$\frac{\partial\rho}{\partial t} + \nabla\cdot\left(\rho\sum_{i=1}^{k} z_i\,\nabla S_i\right) = \frac{\sigma^2}{2}\Delta_x\rho\,, \tag{61}$$

$$\frac{\partial(\rho z_i)}{\partial t} + \nabla\cdot\left(\rho\sum_{j=1}^{k}\big(c_{ij}+z_i z_j\big)\nabla S_j\right) = \frac{\sigma^2}{2}\Delta(\rho z_i) + \rho\kappa_i(\hat{\zeta}_i(S) - z_i)\,. \tag{62}$$

For more details see [39]. In [38] this system of moments with minor modifications is used to simulate the experiments published in [13].

Figure 2(b) shows ρ in a steady state computed by discretization of the system of moments (61), (62).

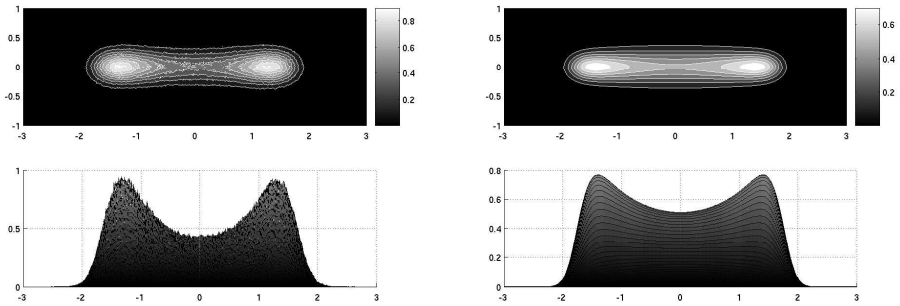

(a) Steady state solution of the stochastic differential equations.

(b) Steady state solution of the system of moments.

FIGURE 2. Comparison of stationary solutions for $\rho(x,t)$.

The covariance matrix C has been computed by averaging the result of the direct simulation 2(a). The differences between Figures 2(a) and 2(b) are explained by the fact that local variations in the (co)variances have been neglected.

6. Modelling of Dictyostelium discoideum

Staying within the framework discussed in the introduction, we assume that the cell density evolves according to the master equation (11), where S is now the external cAMP concentration, and the components of $\zeta \in \mathbb{R}^2$ can be interpreted as the concentration of two internal chemicals, one stimulating the production of the chemoattractant, the other inhibiting it. We assume that the activating chemical, ζ_1, evolves on a very fast time scale and adapts instantaneously such that

$$\zeta_1 = (\bar{z} + h(S) - \zeta_2)_+. \tag{63}$$

Here, h is a sub-linearly increasing function of S and $\bar{z} \geq 0$ a constant. To ensure that ζ_1 is always positive, we take only the positive part on the right hand side of (63). The other variable, ζ_2, evolves slower and aims at restoring the equilibrium value $\bar{z}$ of ζ_1. We set

$$\dot{\zeta_2} = \frac{1}{\tau_z}(h(S) - \zeta_2). \tag{64}$$

Finally, we assume that S is subject to diffusion as well as natural degradation, and that its production rate is proportional to the total concentration of ζ_1,

$$S_t = \Delta S + \rho\zeta_1 - g(S), \tag{65}$$

where $g \geq 0$ is an at least linearly increasing function of S describing its degradation. This system, first introduced in Othmer and Schaap [32], features a typical activator-inhibitor mechanism: the activator ζ_1 grows quickly, stimulates production of S until the inhibitor ζ_2 becomes large enough to slow down the growth of ζ_1 and thus of S and the degradation term $g(S)$ can dominate. Depending on the choice of parameters, this system can both imitate the periodic oscillations of pacemaker cells and the relay behavior of normal cells (see [10]).

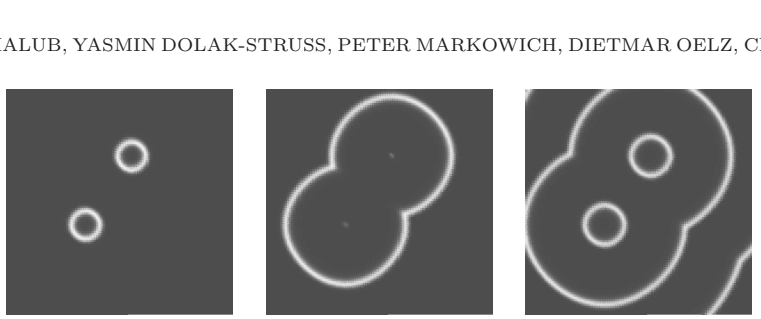

FIGURE 3. Time sequence of cAMP waves on a square domain.

Furthermore, we assume that the evolution of the cell density $P(x, v, \zeta_1, \zeta_2, t)$ is given by (11) and choose a turning kernel satisfying assumption (47) from section 2. The fact that it is a monotonically decreasing function of the material derivative of the chemoattractant, $S_t + v \cdot \nabla S$, can be interpreted such that a cell encountering a rising concentration along its path is less likely to change its direction and the other way round.

Elimination of the equation for ζ_1 and applying a moment closure to (11) similarly to the one shown in the introduction yields a system for $f(x, v, t)$ and $z(x, t)$, the mean value of ζ_2. Finally, carrying out a Chapman-Enskog expansion according to section 2 yields the macroscopic system

$$\rho_t + \nabla_x \cdot (\rho u_c) = \varepsilon \nabla_x \cdot (D \nabla_x \rho) \tag{66}$$

$$(\rho z)_t + \nabla_x \cdot (z \rho u_c) = \varepsilon \nabla_x \cdot (D z \nabla_x \rho) + \frac{h(S) - z}{\tau_z} \tag{67}$$

$$S_t = \Delta S + \left[h(S) - z + \bar{z}\right]_+ \rho - g(S) \tag{68}$$

The chemotactic velocity is of the form $u_c = \chi \nabla S$, where χ is positive and an increasing function in S_t. Note that the diffusion term in (67) differs from that in (31), which is due to a different closure assumption. The derivation of system (66–68) is presented in detail in [10].

Figure 3 and 4 show numerical solutions of the model. For the simulations, we assumed that there are two different types of cells: normal cells with a set of parameters that yield the relay behavior as described above, and pacemakers, with parameters yielding periodic oscillations of the chemical. As initial condition, we put two small discs of pacemaker cells onto a lawn of normal, relay-competent cells. In figure 3, the temporal evolution of the chemoattractant S, spreading in concentric rings is shown. Figure 4 shows a time sequence of the cell density ρ. In contrast to numerical experiments where the chemotactic sensitivity is constant (see [10]), aggregation of cells at the sites of the pacemakers can be observed here.

ACKNOWLEDGMENT

This work has been supported by the Austrian Science Fund (FWF) through the WITTGENSTEIN AWARD 2000 of Peter Markowich, through the Wissenschaftskolleg 'Differential Equations' (project no. W8), and through FWF-Project no. P17139-N04 'Cubature on Wiener Space'. FACCC has been supported by the project POCTI/ISFL/209 (FCT/Portugal) and by the Wolfgang Pauli Institute.

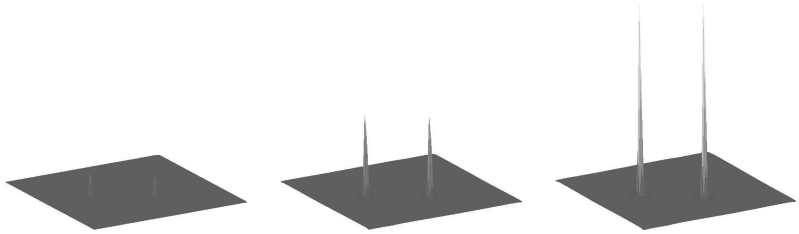

FIGURE 4. Numerical solution of (66), showing the cell density at three different time levels.

REFERENCES

[1] W. Alt. Biased random walk models for chemotaxis and related diffusion approximations. *J. Math. Biol.* 9(2):147-177, 1980

[2] Anderson, A. R. A. and Chaplain, M. A. J. (1997). A Mathematical Model for Capillary Network Formation in the Absence of Endothelial Cell Proliferation. App. Math. Letters, 11: 109-114.

[3] P. Biler. Global solutions to some parabolic-elliptic systems of chemotaxis. *Adv. Math. Sci. Appl.*, 9(1):347–359, 1999

[4] F.A.C.C. Chalub, P.M., B. Perthame and C. Schmeiser. Kinetic models for chemotaxis and their drift-diffusion limits. *Monatsch. Math.*, 142(1-2):123–141, 2004

[5] F.A.C.C. Chalub and J.F. Rodrigues. Kinetic models for chemotaxis with threshold. Preprint.

[6] F.A.C.C. Chalub and K. Kang Global convergence of a kinetic model for chemotaxis to a perturbed Keller-Segel model. Accpeted for *Nonlinear Analysis*.

[7] L. Corrias, B. Perthame, H. Zaag. Global solutions of some chemotaxis and angiogenesis systems in higher space dimensions. *Milan J. Math.* 72:1–28, 2004

[8] R.B. Dickinson and R.T. Tranquillo. Transport equations and indices for random and biased cell migration based on single cell properties. SIAM J. Appl. Math. 55:1419-1454, 1995

[9] R.B. Dickinson and R.T. Tranquillo. A stochastic model for cell random motility and haptotaxis based on adhesion receptor fluctuations. J. Math. Biol. 31:563-600, 1993

[10] Y. Dolak and C. Schmeiser. Kinetic models for chemotaxis: Hydrodynamic limits and the back-of-the-wave problem. *to appear in* J. Math. Biol., 2005

[11] Y. Dolak and C. Schmeiser. The Keller-Segel model with logistic sensitivity function and small diffusivity. *to appear in* SIAM J. Appl. Math., 2005

[12] J. Dolbeault and B. Perthame. Optimal Critical Mass in the two dimensional Keller-Segel model in $\mathbb{R}^2$. C. R. Acad. Sci. Paris, Ser I 339:611-616, 2004

[13] E.F. Foxman, J.J. Campbell and E.C. Butcher. Multistep navigation and the combinatorial control of leukocyte chemotaxis. J. Cell Biol. 139:1349-1360, 1997

[14] J. Geiger, D. Wessels and D.R. Soll. Human Polymorphonuclear Leukocytes respond to waves of chemoattractant, like *Dictyostelium*. Cell Motil. Cytoskeleton, 56:27-44, 2003

[15] M. A. Herrero, E. Medina, and J. J. L. Velázquez. Finite-time aggregation into a single point in a reaction-diffusion system. *Nonlinearity*, 10(6):1739–1754, 1997

[16] M. A. Herrero and J. J. L. Velázquez. A blow-up mechanism for a chemotaxis model. *Ann. Scuola Norm. Sup. Pisa Cl. Sci. (4)*, 24(4):633–683, 1997

[17] T. Hillen and H.G. Othmer. The diffusion limit of transport equations derived from velocity jump processes. SIAM J. Appl. Math. 61(3):751-775, 2000

[18] T. Hillen and K. Painter. Global existence for a parabolic chemotaxis model with prevention of overcrowding. *Adv. in Appl. Math.*, 26(4):280–301, 2001

[19] T. Hillen, K. Painter, and C. Schmeiser. Global Existence for Chemotaxis with Finite Sampling Radius. in preparation, 2005

[20] T. Höfer, J.A. Sherratt and P.K. Maini. Cellular pattern formation during *Dictyostelium* aggregation. Physica D 85:425–444, 1995

[21] D. Horstmann. From 1970 until present: the Keller-Segel model in chemotaxis and its consequences. I. *Jahresber. Deutsch. Math.-Verein.*, 105(3):103–165, 2003

[22] H. J. Hwang, K.Kang and A. Stevens. Drift-diffusion limits of kinetic models for chemotaxis: a generalization. *Discrete Contin. Dyn. Syst. Ser. B*, 5(2): 319–334, 2005
[23] H. J. Hwang, K. Kang and A. Stevens. Global solutions of nonlinear transport equations for chemosensitive movement. *SIAM J. Appl. Math.* 36(4).1177–1199, 2005
[24] E. Ionides, K. Fang, R. Isseroff and G.F. Oster. Stochastic models for cell motion and taxis. J. Math. Biol. 48(1):23-37, 2004
[25] E. Keller and L.A. Segel. Initiation of Slime Mold Aggregation Viewed as an Instability. J. Theor. Biol. 26:399-415, 1970
[26] P. A. Markowich, C. A. Ringhofer, C. Schmeiser. Semiconductor Equations, *Springer Verlag*, Vienna 1990
[27] D. Morale, V. Capasso and K. Oelschläger. An interacting particle system modelling aggregation behavior: from individuals to populations. J. Math. Biol. 50(1):49–66, 2005
[28] T. Nagai. Global existence of solutions to a parabolic system for chemotaxis in two space dimensions. In *Proceedings of the Second World Congress of Nonlinear Analysts, Part 8 (Athens, 1996)*, volume 30, pages 5381–5388, 1997
[29] T. Nagai. Blowup of nonradial solutions to parabolic-elliptic systems modeling chemotaxis in two-dimensional domains. *J. Inequal. Appl.*, 6(1):37–55, 2001
[30] H.G. Othmer, S.R. Dunbar and W. Alt. Models of dispersal in biological systems. J. Math. Biol. 26:263-298, 1988
[31] H.G. Othmer and T. Hillen. The Diffusion Limit of Transport Equations II: Chemotaxis Equations. SIAM J. Appl. Math. 62(4):1222-1250, 2002
[32] H.G. Othmer and P. Schaap. Oscillatory cAMP Signaling in the Development of *Dictyostelium discoideum*. Comm. Theor. Biol. 5:175-282, 1998
[33] K. Painter and T. Hillen. Volume-Filling and Quorum Sensing in Models for Chemosensitive Movement. Canad. Appl. Math. Quart. 10(4):280-301, 2003
[34] C.S. Patlak. Random Walk with Persistence and External Bias. Bull. Math. Biophys. 15:311-338, 1953
[35] B. Perthame. PDE models for chemotactic movements: parabolic, hyperbolic and kinetic. Appl. Math. **49** (2004), no. 6, 539–564;
[36] A.J. Perumpanani, J.A. Sherratt, J. Norbury, H.M. Byrne: Biological inferences from a mathematical model for malignant invasion. Invasion and Metastasis 16: 209-221 (1996).
[37] A.J. Perumpanani, D.L. Simmons, A.J.H. Gearing, K.M. Miller, G. Ward, J. Norbury, M. Schneemann, J.A. Sherratt: Extracellular matrix mediated chemotaxis can impede cell migration. Proc. R. Soc. Lond. B 265: 2347-2352 (1998).
[38] D. Ölz, C. Schmeiser. Multistep navigation of leukocytes: modelling and simulation of in-vitro experiments. Preprint
[39] D. Ölz, C. Schmeiser, A. Soreff. Multistep navigation of leukocytes: a stochastic model with memory effects. *to appear in* Math. Medicine and Biology, 2005
[40] B. Oksendal. Stochastic Differential Equations. Springer-Verlag, 1998.
[41] K. Painter, P.K. Maini and H.G. Othmer. Development and applications of a model for cellular response to multiple chemotactic cues. J. Math. Biol. 41:285-314, 2000
[42] A.B. Potapov and T. Hillen. Metastability in Chemotaxis Models. *to appear in* J. Dyn. Diff. Eq. 17, 2005
[43] F. Poupaud. Runaway phenomena and fluid approximation under high fields in semiconductor kinetic theory. ZAMM Z. Angew. Math. Mech. 72(8):359-372, 1992.
[44] W.J. Rappel, P.J. Thomas, H. Levine and W.F. Loomis. Establishing direction during chemotaxis in eukaryotic cells. Biophysical J. 83:1361-1367, 2002
[45] A. Stevens. The Derivation of Chemotaxis Equations as Limit Dynamics of Moderately Interacting Stochastic Many-Particle Systems. SIAM J. Appl. Math.61 (1):183-212, 2004
[46] D.W. Stroock. Some stochastic processes which arise from a model of the motion of a bacterium. Probab. Theory and Related Fields 28: 305-315, 1974
[47] R.T. Tranquillo and D.A. Lauffenburger. Stochastic model of leukocyte chemosensory movement. J. Math. Biol. 25:229-262, 1987
[48] J. J. L. Velázquez. Point Dynamics in a Singular Limit of the Keller-Segel Model 1: Motion of the Concentration Regions. *SIAM J. Appl. Math.*, 64:1198–1223, 2004
[49] D. Wessels, J. Murray and D.R. Soll. Behaviour of *Dictyostelium* Amoebae is regulated primarily by the temporal dynamics of the natural cAMP wave. Cell Motil. Cytoskeleton, 23:145–156, 1992

Centro de Matemática e Aplicações Fundamentais, Universidade de Lisboa, Av. Prof. Gama Pinto 2, 1649-003, Lisboa Portugal, chalub@cii.fc.ul.pt

Johann Radon Institute for Computational and Applied Mathematics, Austrian Academy of Sciences, Altenbergerstr. 69, 4040 Linz, Austria, yasmin.dolak@oeaw.ac.at

Faculty of Mathematics, University of Vienna and Wolfgang Pauli Institute, Nordbergstrasse 15, 1090 Wien, Austria, peter.markowich@univie.ac.at

Faculty of Mathematics, University of Vienna, Nordbergstrasse 15, 1090 Wien, Austria, dietmar.oelz@univie.ac.at

Faculty of Mathematics, University of Vienna Nordbergstrasse 15, 1090 Wien, Austria, Johann Radon Institute for Computational and Applied Mathematics, Austrian Academy of Sciences, Altenbergerstr. 69, 4040 Linz, Austria, christian.schmeiser@tuwien.ac.at

Faculty of Mathematics, University of Vienna Nordbergstrasse 15, 1090 Wien, Austria, a.soreff@tuwien.ac.at